

Complete Valvular Heart Apparatus Model from 4D Cardiac CT

Razvan Ioan Ionasec¹, Sasa Grbic², Dime Vitanovski², Ingmar Voigt, Bogdan Georgescu¹, Fernando Vega-Higuera³, and Dorin Comaniciu¹

¹ Medical Informatics, Siemens Corporate Research, Princeton, USA

² Software and Engineering, Siemens Corporate Technology, Erlangen, Germany

³ Computed Tomography, Siemens Healthcare Sector, Forchheim, Germany

Abstract. The cardiac valvular apparatus, composed of the aortic, mitral, pulmonary and tricuspid valve, is an essential part of the anatomical, functional and hemodynamic characteristics of the heart and the cardiovascular system as a whole. Valvular heart diseases often involve multiple dysfunctions and require joint assessment and therapy of the valves. In this paper, we propose a complete and modular patient-specific model of the cardiac valvular apparatus estimated from 4D cardiac CT data. A new constrained Multi-linear Shape Model (cMSM), conditioned by anatomical measurements, is introduced to represent the complex spatio-temporal variation of the heart valves. The cMSM is exploited within a learning-based framework to efficiently estimate the patient-specific valve parameters from cine images. Experiments on 64 4D cardiac CT studies demonstrate the performance and clinical potential of the proposed method. To the best of our knowledge, it is the first time cardiologists and cardiac surgeons can benefit from an automatic quantitative evaluation of the complete valvular apparatus based on non-invasive imaging techniques. In conjunction with existent patient-specific chamber models, the presented valvular model enables personalized computation modeling and realistic simulation of the entire cardiac system.

1 Introduction

The heart valves are an essential anatomical structure regulating the heart chambers hemodynamics and the blood flow between the heart and the human body. Valvular heart disease (VHD) is a frequent symptom, with a prevalence of 2.5% among the global population often obliged to complex management and therapeutical procedures. Moreover, valve operations are the most expensive and most precarious cardiac interventions, with an average cost of \$141,120 and 4.9% in-hospital death rate in the US [1].

Due to the strong anatomical, functional and hemodynamic inter-dependency of the heart valves, VHDs do not affect only one valve, but rather several valves are impaired. Recent studies demonstrate strong influence of pulmonary artery systolic pressure on the tricuspid regurgitation severity [2]. In [3, 4] the simultaneous evaluation of aortic and mitral valves is encouraged, given the fibrous aortic-mitral continuity, which anchors the left side valves and facilitates the reciprocal opening and closing motion during the cardiac cycle. Moreover, in patients with mitral and tricuspid valve regurgitation, joint surgery is recommended to minimize the risk for successive heart failure or reduced functional capacity. Complex

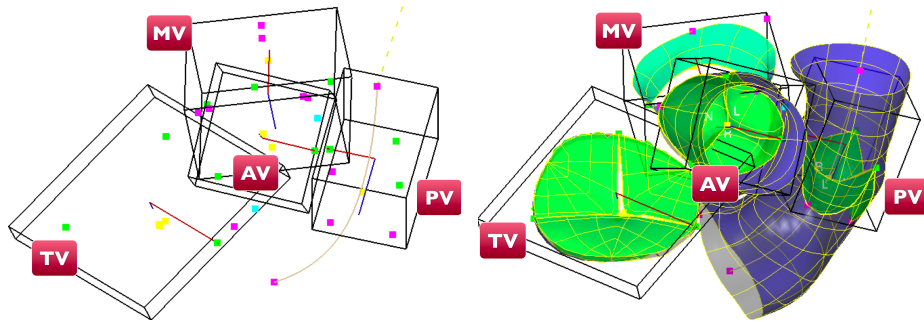


Fig. 1. Complete heart valves model consisting of aortic valve (AV), mitral valve (MV), pulmonary valve (PV) and tricuspid valve (TV). **Left:** Similarity transform illustrated as a bounding box and anatomical landmarks. **Right:** Complete mesh surface model.

procedures mostly performed in patients with congenital heart diseases, such as the Ross operation, in which the aortic valve is replaced with the pulmonary, require comprehensive quantitative and qualitative evaluation of the heart valves. Morphological and Functional Assessment of the complete heart valve apparatus is crucial for clinical decision making during diagnosis and severity assessment as well as treatment selection and planning.

An increased holistic view of the heart, demanded by clinicians is in perfect accordance with the tremendous scientific effort worldwide, such as the Virtual Physiological Human project [5], geared towards multi-scale physiological modeling and simulation, which will promote personalized, preventive and predictive healthcare. However, the majority of cardiac models to date focus on representation of the left or right ventricle [6], while very few include the left and right atrium [7], but none explicitly handles the valves. Recently introduced models of the aortic-mitral coupling [8, 9] do not incorporate the right side valves. A critical component for a patient-specific computation model of the entire heart and realistic cardiovascular simulations, which was not reported yet in the literature, is a personalized and complete representation of the valvular apparatus. In this paper we propose a complete and modular model of the heart valves comprising the anatomy of the aortic, mitral, tricuspid and pulmonary valves as well as their morphological, functional and pathological variations. The patient-specific valvular apparatus is estimated non-invasively from 4D Computed Tomography images, using a discriminative learning-based approach. Global valve location and motion, as well as the non-rigid movement of anatomical valvular landmarks, are computed within the Marginal Space Learning (MSL) [10] and Trajectory Spectrum Learning (TSL) [8] frameworks. A novel anatomical Constrained Multi-linear Shape Model (cMSM) is introduced to capture complex spatio-temporal statistics, and in conjunction with robust boundary detectors, it is applied to extract the complete valvular anatomy and motion. Our approach enables for integrated quantification and treatment management of heart valves,

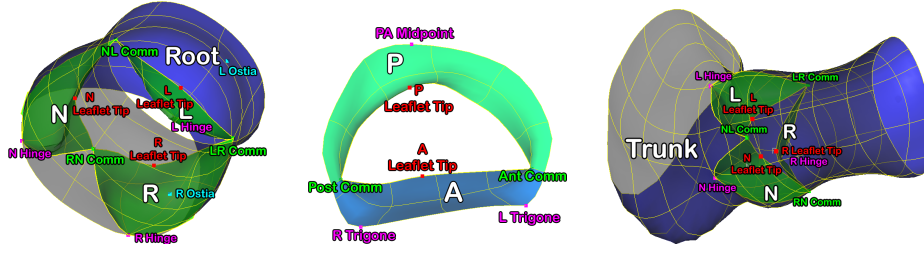


Fig. 2. Anatomical Landmark Model and Complete Valve Model of the aortic valve (left), mitral valve (middle) and pulmonary valve (right).

and together with a patient specific chamber model [10], it will enable comprehensive heart simulations [11].

2 Physiological Model of the Heart Valves

In this section we introduce the complete heart valves model, which includes the aortic, mitral, tricuspid and pulmonary valves, and captures morphological, functional and pathological variations. To reduce anatomical complexity and facilitate effective estimation, the heart valve model is represented on two abstraction layers: Anatomical Landmark Model - which represents the global location and motion of each valve, as well as the motion of the corresponding anatomic landmarks; Complete Valve Model - which parameterizes the full anatomy and dynamics of the valves using dense surface meshes.

Anatomical Landmark Model. The global dynamic variation of each valve is parametrized as a temporal dependent similarity transform (see Fig. 1).

$$\mathbf{B} = \{(x_1, x_2, x_3), (q_1, q_2, q_3), (s_1, s_2, s_3), t\} \quad (1)$$

(x_1, x_2, x_3) is the translation, (q_1, q_2, q_3) the quaternion representation of the rotation, (s_1, s_2, s_3) the similarity transform scaling factors and t the temporal position in the cardiac cycle. A set of 33 anatomical landmarks, described in the next paragraph, are used to parameterize the complex and synchronized motion pattern of all valves, which explains the non-linearities of the hemodynamic movements. Thereby, each landmark is described by a T time-step trajectory in a three dimensional space, normalized by the temporal dependent similarity transform \mathbf{D} :

$$\mathbf{L}_n(\mathbf{B}) = \{l_1, l_2, \dots, l_T\} \quad n \in 1 \dots 33 \quad l_i \in \mathbb{R}^3 \quad (2)$$

Complete Valve Model. The final valves model is completed with a set of 13 dense surface meshes. Each mesh is sampled along anatomical grids of vertices defined through the landmarks:

$$\mathbf{V}_q(\mathbf{L}, \mathbf{B}) = \{\mathbf{v}_1, \mathbf{v}_2, \dots, \mathbf{v}_{K_q}\} \quad q \in 1 \dots 13 \quad \mathbf{v}_i \in \mathbb{R}^3 \quad (3)$$

where v_i are the vertices, and K_q is the total number of vertices of mesh q .

Aortic valve: The aortic valve is constrained by 11 landmarks (3 commissures, 3 hinges, 3 leaflet tips and 2 ostias) and four anatomical structures (aortic root, N-, L- and R-leaflet). The aortic root is constrained by the hinge and commissure plane and each leaflet is spanned between two commissures and one hinge, as in [8], (see Fig. 2 (left)).

Mitral valve: The mitral valve is composed of 7 landmarks (3 trigones, 2 commissures and 2 leaflet tips). The anterior leaflet is defined by two trigones, one leaflet tip and two commissures and the posterior leaflet by three trigones, one leaflet tip and one commissure, as in [8], (see Fig. 2 (middle)).

Pulmonary valve: The pulmonary valve is consisting of 9 landmarks (3 commissures, 3 hinges and 3 leaflet tips) and four anatomical structures (pulmonary root, N-, L- and R-leaflet), as in [8], (see Fig. 2 (right)).

Tricuspid valve: The function of the tricuspid valve is to regulate the blood flow from the right atrium to the right ventricle, staying closed during systole and opened during diastole. The model is constrained by four surface geometries (annulus, septal-, anterior- and posterior leaflet) (Fig. 3) and six anatomical landmarks (three commissures and three leaflet tips) which are corresponding to vertices on the meshes. The tricuspid annulus is represented as a surface mesh constrained by the three commissures. The tricuspid leaflets, the A, S and P, are modeled as hyperbolic paraboloids. The vertices on the leaflet border have fixed correspondences to vertices on the tricuspid annulus. Each leaflet is defined by two commissures and one leaflet tip.

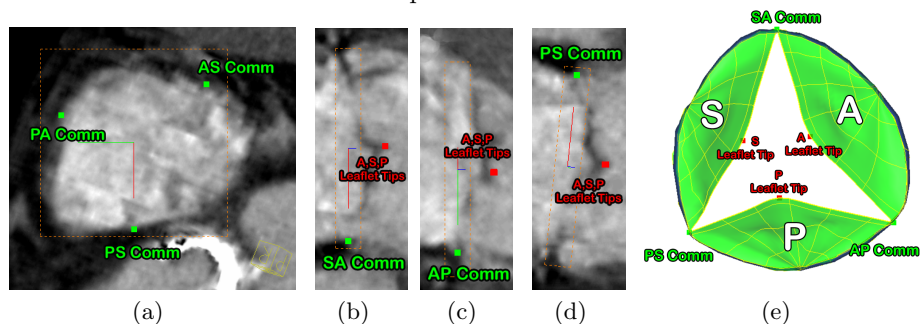


Fig. 3. Tricuspid valve model. (a)-(d) shows anatomical landmarks (commissures and leaflet tips) and (e) is showing the complete surface mesh (annulus and leaflets).

3 Patient-Specific Model Estimation

A hierarchical estimation approach is utilized to deduce model parameters, introduced in the previous section from 4D cardiac CT images. First, robust machine learning techniques are applied to estimate the global valves and anatomic landmarks parameters introduced in Eq. 1 and 2. Second, we present the novel anatomical constrained Multi-linear Shape Model (cMSM), which effectively captures the complex spatio-temporal variation of all valves. Lastly, the cMSM is

applied in a learning-based framework to estimated the complete valve model described in Eq. 3.

3.1 Landmark Location and Motion Estimation

The global motion and landmarks parameters are estimated within the Marginal Space Learning framework [7], similar as in [8].

3.2 Constrained Multi-linear Shape Model

Multilinear modeling enables the decomposition of a shape space in a temporal and spatial component in contrast to active shape models (ASM) where both are coupled. In this paper we present a Multi-linear MPCA (Multi-linear Principle Component Analysis) and MICA (Multi-linear Independent Component Analysis) shape model of all valves which is conditioned by anatomical measurements.

Shape Space. In order to construct the shape model all shapes \mathbf{V} are aligned by calculating the mean sequence model and aligning them using general procrustes analysis (GPA). This transform is utilized to align all shapes in the sequence. The normalized shapes are represented as third-order tensors $\mathbf{D} \in \mathbb{R}^{(S \times T \times P)}$, where S is the number of patients, T is the frame number inside a multi phase sequence and P represents the number of shape points.

$$\mathbf{D} = \mathcal{Z} \times_1 \mathbf{U}_{\text{patient}} \times_2 \mathbf{U}_{\text{motion}} \times_3 \mathbf{U}_{\text{points}}$$

As mentioned by [12] the motion subspace due its non-Gaussian distribution is decomposed using ICA and the patient and points space using PCA.

$$\begin{aligned} \mathbf{D} &= \mathcal{Z} \times_1 \mathbf{U}_{\text{patient}} \times_2 \mathbf{U}_{\text{motion}} \mathbf{W}^{-1} \mathbf{W} \times_3 \mathbf{U}_{\text{points}} \\ &= (\mathcal{Z} \times_2 \mathbf{W}_1) \times_1 \mathbf{U}_{\text{patient}} \times_2 \mathbf{U}_{\text{motion}} \mathbf{W}^{-1} \times_3 \mathbf{U}_{\text{points}} \\ &= \mathcal{S} \times_1 \mathbf{U}_{\text{patient}} \times_2 \mathbf{C}_{\text{motion}} \times_3 \mathbf{U}_{\text{points}} \end{aligned}$$

Constrained Model Estimation. A set of anatomical measurements $\mathbf{M} (m_1, m_2, \dots, m_R)$ extracted from the non-linear valve model is used to condition a surface parameterization $\mathbf{V}_q (\mathbf{v}_1, \mathbf{v}_2, \dots, \mathbf{v}_{K_q})$ [13]. Assuming the joint multivariate distribution $(\mathbf{V}_q | \mathbf{M})$ follows a Gaussian distribution a conditioned surface \mathbf{V}_q^M , containing the anatomical measurements \mathbf{M} , can be estimated as follows:

$$\mathbf{V}_q^M = \mu_{\mathbf{V}_q} + \Sigma_{\mathbf{V}_q \mathbf{M}} \Sigma_{\mathbf{M} \mathbf{M}}^{-1} (\mathbf{M} - \mu_{\mathbf{M}})$$

where $\mu_{\mathbf{V}_q}$ is the mean surface parameterization from all training sets of the valve surface \mathbf{V}_q , $\mu_{\mathbf{M}}$ the mean of the measurements \mathbf{M} in the training set, $\Sigma_{\mathbf{V}_q \mathbf{M}}$ the covariance matrix between \mathbf{V}_q and \mathbf{M} . The constrained surface \mathbf{V}_q^M is used to reconstruct the dynamic motion surface model of the whole sequence. Therefore we first estimate the patient modes $\mathbf{u}_{\text{patient}}$ and then use them to reconstruct $\mathbf{V}_q (\mathbf{L}, \mathbf{D})$.

$$\mathbf{u}_{\text{patient}} = \mathbf{V}_q^M \mathbf{T}_{(1)}^{-1} \quad \mathcal{T} = \mathcal{S} \times_2 \mathbf{C}_{\text{motion}} \times_3 \mathbf{U}_{\text{points}}$$

where $\mathbf{T}_{(1)}^{-1}$ is the pseudo-inverse of the tensor \mathcal{T} flattened along the first mode and $\mathbf{C}_{\text{motion}}$ the one dimensional motion mode. The complete surface model for the complete sequence, introduced in Eq. 3, can be extracted by a tensor multiplication:

$$\mathbf{V}_q(\mathbf{L}, \mathbf{D}) = \mathcal{S} \times_1 \mathbf{u}_{\text{patient}} \times_2 \mathbf{C}_{\text{motion}} \times_3 \mathbf{U}_{\text{points}}$$

3.3 Complete Valve Model Estimation

The comprehensive surface model $\mathbf{V}_q(\mathbf{L}, \mathbf{D})$ of each anatomical structure q , is estimated by adopting the constrained Multi-linear shape method using anatomical measurements \mathbf{M} defined between the landmarks $\mathbf{L}_1 \cdots \mathbf{L}_K$. E.g. for the aortic root we use three measurements $\mathbf{M} = \{m_1, m_2, m_3\}$ (m_1 -inter-commissure distance, m_2 -hinge-commissure plane distance, m_3 -hinge-commissure plane angle). The shape prediction \mathbf{V}_q is locally refined using a boundary detector, trained using PBT [14] and Steerable features [15].

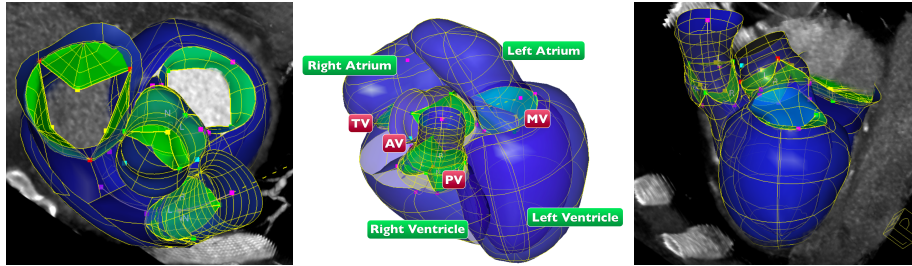


Fig. 4. Examples of estimated personalized model from a multiphase CT sequence.

4 Experimental Results

The accuracy of the proposed method was evaluated using 64 multi phase CT data sets, containing 640 volumes. The data sets comprise a variety of cardiovascular diseases and due to different acquisition protocols they have heterogeneous image quality, resolution and sizes. For every study ground-truth annotations are provided by an expert user. Each evaluation is done using three-fold cross validation.

The estimation of the Anatomical Landmark Model is performed in two stages. First the global dynamic motion is evaluated by the Euclidian distance between the corner points of the ground-truth and estimated box in each frame. Second, the non-linear landmark model error is computed as the mean Euclidian distance of all detected landmarks compared to the expert annotation. The complete valve model, containing the dense surface meshes, is measured as the mesh-to-mesh distance. Results shown in table 1 corroborate that our constrained ML PCA-ICA shape estimation approach achieves best performance, compared to a regular ML PCA-ICA method and a standard frame-wise estimation procedure

(tracking by detection). Within four minutes a complete personalized dynamic model of all valves is estimated with an average accuracy of 1.24 mm. The full valvular model together with the four chambers of the heart is illustrated in Fig. 4. Important clinical parameters are extracted from the personalized model in

Table 1. System precision for valve model estimation averaged on all valves. **Left:** Evaluation of the Anatomical Landmark Model. **Right:** Comprehensive Surface assessment.

	Mean	STD	Median
Similarity T. [mm]	5.67	2.36	5.29
Landmark Motion [mm]	2.61	1.17	2.41

	Mean	STD	Median
Tracking by Detection [mm]	1.52	0.98	1.47
ML PCA-ICA [mm]	1.39	0.91	1.32
cML PCA-ICA [mm]	1.24	0.91	1.18

the right heart. They include right-ventricle outflow tract (RVOT) radius, Bifurcation radius, tricuspid valve area and a joint measurement of the two valves, the pulmonary and tricuspid valve distance. Quantitative comparison is shown in Fig. 5 by comparing ground truth measurements and the estimated, demonstrating a strong correlation.

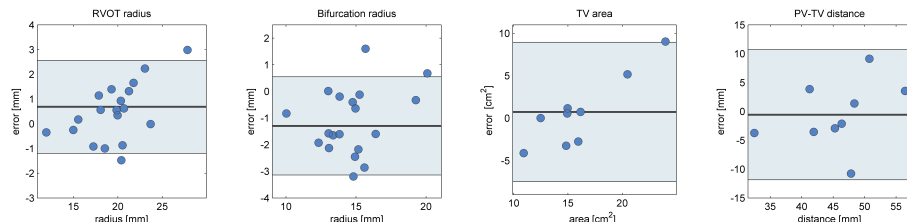


Fig. 5. Bland altman plots for a) right ventricle output tract diameter, b) pulmonary valve bifurcation diameter, c) tricuspid valve area and d) distance between pulmonary and tricuspid valve

Finally we show quantitative comparison between a healthy patient and a post-operative patient who underwent a Ross operation. Several clinical measurements extracted from the personalized aortic and pulmonary valve model, demonstrated in Fig. 6), confirm a successful outcome since no regurgitation is observed at the aortic valve.

5 Conclusion

In this paper, we propose a novel personalized model for quantitative and qualitative evaluation of the complete heart valve apparatus in 4D CT. It is capable to delineate the full anatomy and dynamics needed to depict a large variation of valve pathologies, especially diseases affecting several valves. Its hierarchical approach using state of the art machine learning algorithms in combination with

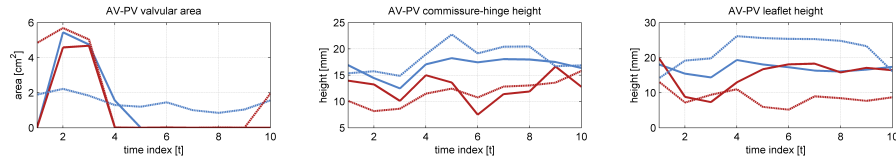


Fig. 6. Measurements (**left:** aortic (AV) and pulmonary valve (PV) area, **middle:** mean commissure-hinge plane height and **left:** mean leaflet height) obtained from a normal patient (solid lines) and a post Ross operation patient (dotted line). The red graph is representing the aortic valve and the blue the pulmonary.

a constrained Multi-linear shape space enables an patient specific model estimation within three minutes and an accuracy of 1.24 mm. Clinical validation shows strong correspondence between expert- and model estimated anatomical measurements. The proposed method could spark research in many areas such as examining interconnections of multiple valves and hemodynamic simulation of the complete cardiac apparatus.

References

1. Lloyd-Jones, D., et al.: Heart disease and stroke statistics–2009 update: a report from the american heart association statistics committee and stroke statistics subcommittee. *Circulation* **119** (2009) 21–181
2. Mutlak, D., et al.: Functional tricuspid regurgitation in patients with pulmonary hypertension. *CHEST* (2009) 115–121
3. Lansac, E., et al.: Dynamic balance of the aortomitral junction. *J Thorac Cardiovasc Surg* **123** (2002) 911–918
4. Timek, T., et al.: Aorto-mitral annular dynamics. *Ann Thorac Surg* **76** (2003) 1944–1950
5. Clapworthy, G., et al.: Editorial. *Philosophical Transactions of the Royal Society A: Mathematical, Physical and Engineering Sciences* **366**(1878) (2008) 2975–2978
6. Fritz, D., et al.: Segmentation of the left and right cardiac ventricle using a combined bi-temporal statistical model. In: *SPIE Medical Imaging*. (2006) 605–614
7. Zheng, Y., et al.: Four-chamber heart modeling and automatic segmentation for 3d cardiac ct volumes using marginal space learning and steerable features. *IEEE TMI* **27**(11) (2008) 1668–1681
8. Ionasec, R.I., et al.: Personalized Modeling and Assessment of the Aortic-Mitral Coupling from 4D TEE and CT. In: *MICCAI, Heidelberg* (2009) 767–775
9. Veronesi, F., et al.: A study of functional anatomy of aortic-mitral valve coupling using 3D matrix transesophageal echocardiography. *Circ Cardiovasc Imaging* **2**(1) (2009) 24–31
10. Zheng, Y., et al.: Fast automatic heart chamber segmentation from 3d ct data using marginal space learning and steerable features. In: *ICCV*. (2007)
11. Mihalef, V., et al.: Patient-specific modeling of left heart anatomy, dynamics and hemodynamics from high resolution 4d ct. In: *ISBI*. (2010)
12. Zhu, Y., et al.: A dynamical shape prior for lv segmentation from rt3d echocardiography. In: *MICCAI*. (2009)
13. Blanc, R., et al.: Conditional variability of statistical shape models based on surrogate variables. In: *MICCAI*. (2009)

14. Tu, Z.: Probabilistic boosting-tree: Learning discriminative methods for classification, recognition, and clustering. In: ICCV. (2005) 1589–1596
15. Freeman, W.T., Adelson, E.H.: The design and use of steerable filters. *IEEE Trans. Pattern Anal. Machine Intell.* **13**(9) (1991) 891–906